Journal of Colloid and Interface Science 503 (2017) 68–75

Contents lists available at ScienceDirect

Journal of Colloid and Interface Science

journal homepage: www.elsevier.com/locate/jcis

Regular Article

Direct exfoliation of graphite in water with addition of ammonia solution

Han Ma [a,b], Zhigang Shen [a,b,*], Min Yi [c], Shuang Ben [d], Shuaishuai Liang [e], Lei Liu [b], Yixiang Zhang [b], Xiaojing Zhang [b], Shulin Ma [b]

[a] School of Materials Science and Engineering, Beihang University, Beijing 100191, China
[b] Beijing Key Laboratory for Powder Technology Research and Development, Beihang University, Beijing 100191, China
[c] Institute of Materials Science, Technische Universität Darmstadt, Darmstadt 64287, Germany
[d] School of Chemistry and Environment, Beihang University, Beijing 100191, China
[e] State Key Laboratory of Tribology, Tsinghua University, Beijing 100084, China

GRAPHICAL ABSTRACT

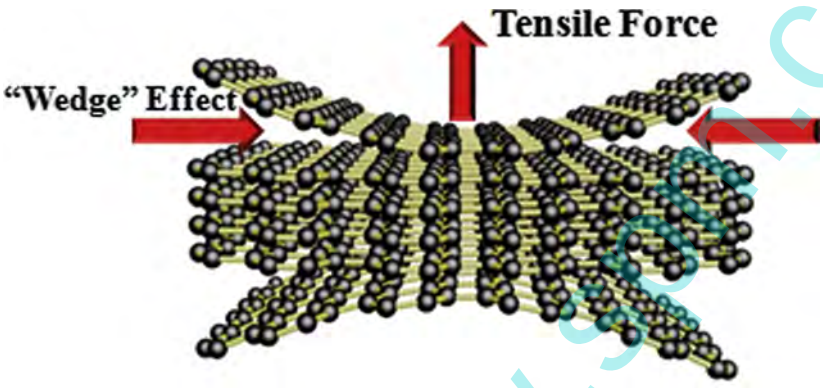

ARTICLE INFO

Article history:
Received 9 December 2016
Revised 18 April 2017
Accepted 22 April 2017
Available online 24 April 2017

Keywords:
Graphene
Exfoliation
Water
Ammonia solution

ABSTRACT

To bring graphene closer to its real-world applications, finding a green, low-cost, environment-friendly and less toxic solvent for production of high-quality graphene is highly demanded. However, water, the most widely used green solvent, is generally considered to be a poor solvent for hydrophobic graphene. In this study, we exfoliate graphene nanosheets directly in basic water without surfactants, polymers or organic solvents. The addition of a small amount of ammonia solution achieves the exfoliation of few-layer graphene nanosheets from pristine graphite. Diverse characterization methods are employed to investigate the morphology and quality of as-prepared graphene sheets. The release of gaseous ammonia plays the key role in exfoliation of graphene. The concentration of stable graphene dispersions can reach 0.058 mg/mL.

* Corresponding author at: School of Materials Science and Engineering, Beihang University, Beijing 100191, China.
E-mail addresses: hawkinsma1218@gmail.com (H. Ma), shenzhg@buaa.edu.cn (Z. Shen), minyibhu@gmail.com (M. Yi), 347872954@qq.com (S. Ben), doubleleung@sina.com (S. Liang), liulei0111@qq.com (L. Liu), buaazyx@hotmail.com (Y. Zhang), zhangxiaojing@buaa.edu.cn (X. Zhang), mshl@buaa.edu.cn (S. Ma).

http://dx.doi.org/10.1016/j.jcis.2017.04.070
0021-9797/

1. Introduction

Graphene, one kind of two-dimensional nanomaterial, has attracted much attention in a series of application fields. Constituted by the honeycomb C—C network, graphene possesses extraordinary mechanical [1], electronic [2], thermal [3] and optical properties [4], and thus holds great promise in a wide range of applications including energy storage [5], composite [6] and catalysis [7]. However, despite its huge potential and bright prospects, the scalable production of graphene remains a huge challenge.

The common methods for preparation of graphene mainly include micromechanical cleavage [8], chemical vapor deposition (CVD) [9], epitaxial growth [10], reduction of graphene oxide [11] and liquid exfoliation of graphite [12,13]. Among them, reduction of graphene oxide (GO) is typically regarded as the strategy that is most suitable for mass production of graphene. GO can be easily dispersed in water to form stable colloids owing to abundant oxygenated functional groups attached to its basal plane and edges [14]. After the reduction process, GO can be converted to reduced graphene oxide (RGO) as these groups are eliminated. However, this approach has its own disadvantages. Though oxidation-reduction method can achieve high graphene concentrations, the reduction process is not green for the usage of highly toxic reducing agents like hydrazine [15], and reactions at an extremely high temperature [11]. Besides, the oxygen-contained functional groups, which make GO electrically insulate, cannot be reduced completely [14]. The residual defects after reduction also render the properties of as-prepared RGO inferior to those of pristine graphene.

In contrast, liquid exfoliation of graphite in suitable solvents provides a simple and cost-efficient route to graphene preparation. Specifically, the Van der Waals force between graphite internal layers is overcome by applied mechanical interactions, e.g. ultrasonic cavitation [16]. Significantly, such method can maintain the structural integrity of pristine graphene to a large extent, and thus outperform the oxidation-reduction method. However, liquid exfoliation is not without drawbacks. It has been demonstrated that organic solvents, like NMP [12] and DMF [17], are excellent solvents for producing graphene due to their suitable surface energy, but they suffer from high cost, toxicity, high boiling point and a lack of user-friendliness, etc. On the other hand, to exfoliate graphite in aqueous solutions, surfactants are often introduced to stabilize graphene suspensions, as depicted in many reports [18,19]. Such surfactants or organic solvents are quite difficult to eliminate completely, thus exerting negative effects on the properties that make graphene unique. To solve this problem, searching green, volatile and low-cost solvents for preparing graphene is of great importance.

Water is the most common and widely used solvent that offers advantages such as low boiling point and good environmental compatibility. Unfortunately, it is well known that water is a poor solvent for graphene due to its hydrophobic nature. Recently, significant efforts have been devoted on this issue. To maximize the surface charge, Li et al. [20] used ammonia solution to modulate the pH value, resulting in stable aqueous dispersions of chemical converted graphene (CCG) with a high concentration of ~0.5 mg/mL without the assistance of polymers or surfactants, but this method still suffers from the highly toxic hydrazine. Yi et al. [21] demonstrated that graphene produced by liquid exfoliation in organic solvent can be stably dispersed in pure water. Additionally, smaller graphene flakes results in more stable dispersion. Generally, both works proved possible dispersability of graphene in aqueous environment based on electrostatic repulsion between flakes. Furthermore, some researchers attempt to directly exfoliate pristine graphite in water. For example, Ricardo et al. [22] prepared multilayer graphene by directly exfoliating graphite in the aqueous solution of NaOH, but the maximum value of graphene concentration was only 0.02 mg/mL. Kim et al. [23] achieved direct exfoliation of graphite and storage of graphene nanosheets in pure water via temperature control (333 K), but the concentration of graphene only reached 7.5 μg/ml after a quite long sonication process (60 h). Therefore, scalable production of graphene nanosheets in water still remains a big challenge.

In this work, to prepare water-dispersed graphene, we propose a facile, green, cost-efficient and in situ approach, in which the addition of a small amount of ammonia solution allows for exfoliation of graphite in water. We find that graphite can be exfoliated to few-layered graphene nanosheets, while the use of organic solvents, polymers and surfactants is not required. The volatile nature of aqueous ammonia makes it easy to evaporate during the processing of the graphene dispersion. Our findings not only offer new options of solvents for liquid exfoliation, but also pave the way for scalable production of graphene in water-based systems.

2. Experimental

2.1. Materials

The pristine graphite powder was purchased from Alfar Aesar (325 mesh, Product Number 43209). The deionized (DI) water was obtained from Beijing Kebaiao Biotech. Co., Ltd. The ammonia solution (25–28%) was bought from Xilong Chemical Co., Ltd. All the materials were used as received.

2.2. Preparation of graphene

The schematic process flow is shown in Fig. S1. In a typical experiment, 200 mL of DI water was poured into a wide-mouth bottle with the volume of 500 mL, in which 40 μL of aqueous solution of ammonia was utilized to adjust the pH value to around 9. 4000 mg of graphite powder was added into the basic water to achieve an initial concentration of 20 mg/mL. The mixture of graphite and water was sonicated for 2 h at a fixed position in one sonic bath (1730 T, 120 W, 40 kHz, Beijing Kexi Ultrasonic Instrument Co., Ltd., China). During the sonication process, a piece of preservative film was covered on the sealed cap of the bottle to prevent ammonia evaporation. After sonication, the as-prepared dispersion was allowed to stand for 2 h. Then the upper dispersion was centrifuged at 2000 rpm for 30 min with a 80-2 Centrifuge (Jintan Zhongda Apparatus Co., Ltd., China) to remove large flakes and unexfoliated graphitic particles. Eventually, the supernatant of the centrifugation tubes was carefully assembled as the graphene dispersion. A thin film of graphene was prepared via vacuum filtration of the graphene dispersion through a porous membrane (mixed cellulose esters, pore size 0.22 μm). Parameters mentioned above, including pH value, sonication time, initial concentration of graphite and centrifugation rate, were altered to investigate effects of them. All of the experiments were performed at ambient conditions.

2.3. Characterization

Transmission electron microscope (TEM) and high-resolution TEM (HRTEM) images were taken with a JEOL 2100 operating at 200 kV. TEM samples were prepared by pipetting a few drops of dispersions onto holey carbon grids. Atomic force microscope (AFM) analyses were performed using a CSPM5500 (Beijing Nano-Instruments Ltd., China) to investigate thickness and lateral size of graphene. AFM samples were prepared by pipetting several microliters of graphene dispersion onto mica substrates. The concentration of graphene, C, was calculated following Lambert-Beer

law, A/l = αC, where α was regarded as 2460 mg/mL/m [12]. The optical absorbance, A, was measured at 660 nm using 1 cm quartz by a UV–vis spectrophotometer (Purkinje General TU1901). The Raman and X-ray photoelectron spectroscopy (XPS) samples were the graphene films prepared via vacuum filtration. Raman analyses were conducted using a Renishaw Rm2000 with a 514 nm laser. XPS was carried out using a Thermo Fisher Scientific ESCALAB-250 spectrometer. Zeta potential measurements were performed on a Malvern Zetasizer 3000HSa apparatus. XRD patterns were collected by using Cu Kα radiation with an X-ray diffractometer (Bruke D8-advance). FTIR spectra were measured using a Nicolet iS10 spectrometer. All of characterizations were done at 25 °C.

3. Results and discussion

3.1. Tailoring the parameters

Aqueous ammonia was used to modulate the pH value from 8 to 11. As can be seen in Fig. 1a, using pure water as the solvent resulted in an almost transparent and colorless dispersion, and thus an extremely low concentration of graphene. In contrast, by adding a very small amount of ammonia solution, a dark dispersion could be obtained. The concentration of graphene (pH = 9) reached 28.94 μg/mL, which was 20 times higher than that using pure water. For comparison, after sonication (prior to the centrifugation step), the dark dispersions with and without pH adjustment were also sedimented for 48 h. As shown in Fig. S2, we found that for the sample using pure water, the upper dispersion turned to be entirely transparent with a small amount of visible graphitic particles suspended. This indicates a low extent of exfoliation or high level of precipitation. Interestingly, the sample with pH adjustment appeared dark and homogeneous. This phenomenon can be attributed to the efficient exfoliation of graphite. We also investigated the effects of the amount of ammonia solution. We found that a weakly alkaline environment, in which the pH value ranges from 9 to 11, favors the exfoliation of graphite, as seen in Fig. 1b. In addition, it is found that the as-prepared graphene colloids are stable, as no severe sedimentation occurred within several weeks. Zeta potential (Fig. 1b) suggests that the as-prepared graphene nanosheets are stabilized via electrostatic repulsion [20–22].

For the liquid exfoliation strategy, the initial concentration (C) of graphite and the sonication time (t_s) are of great importance to the final concentration of graphene (C_G). In this study, we also investigated the effects of these two parameters. It was found that

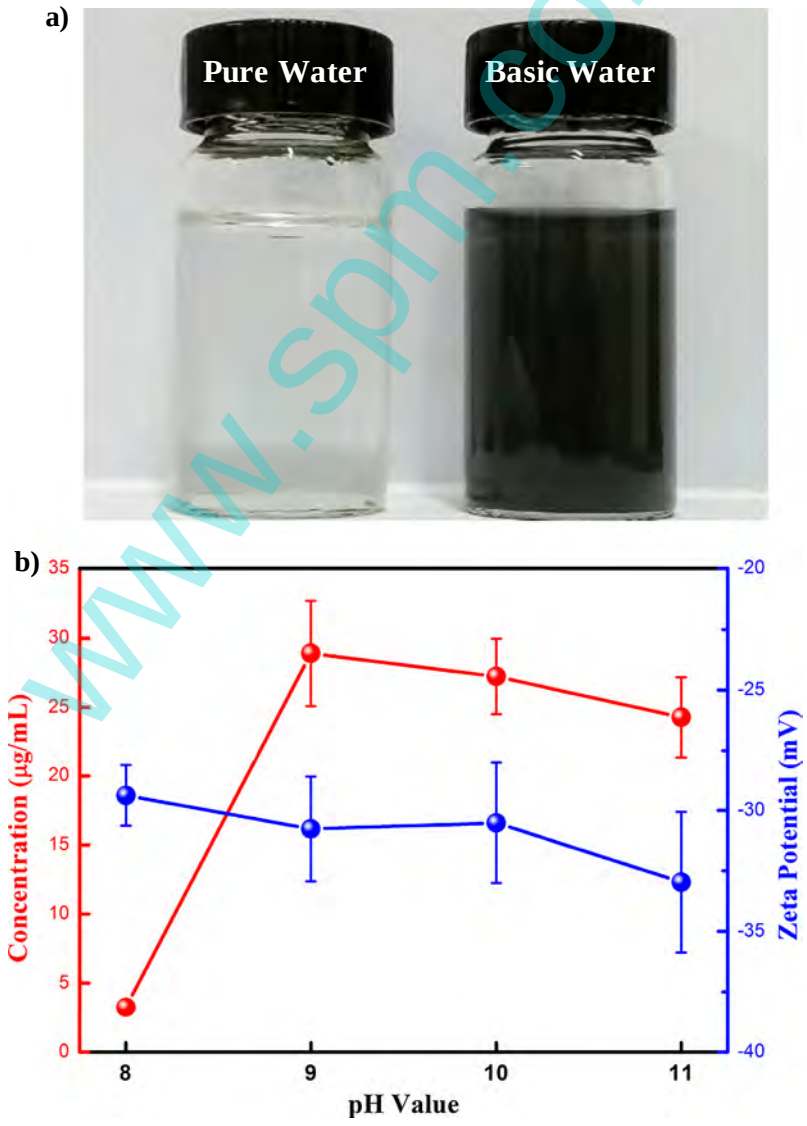

Fig. 1. (a) Graphene dispersions prepared in pure water and basic water. (b) Concentration and zeta potential of graphene dispersions as a function of pH value.

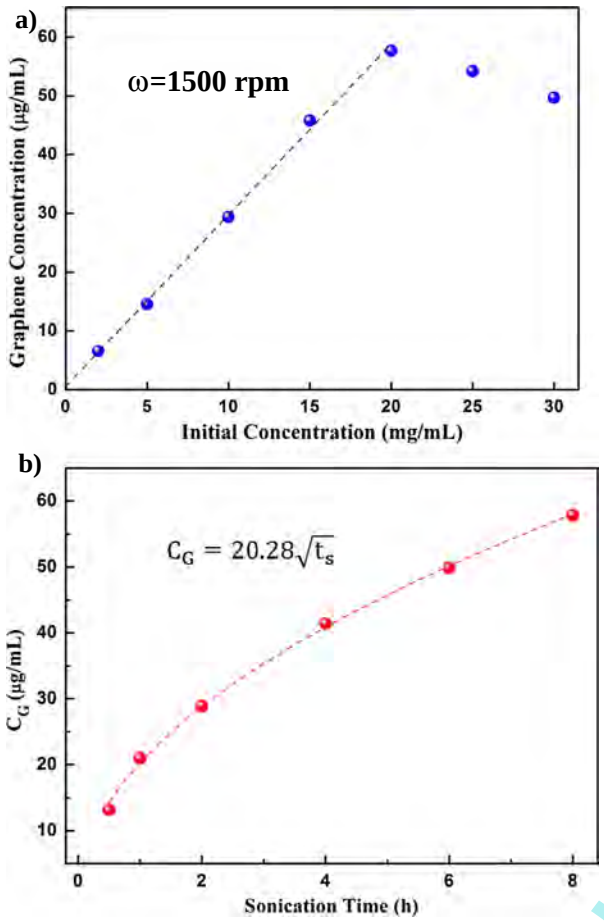

Fig. 2. Graphene concentration as a function of initial concentration of pristine graphite (a) and sonication time (b).

the concentration of graphene approximately scales with C (for C < 20 mg/mL) and $\sqrt{t_s}$, respectively, as shown in Fig. 2a and b. This conclusion is in good accordance with that reported by Coleman's group [24,25]. It can be seen that C_G reaches a value of ~58 μg/mL when the sonication time is extended to 8 h. This value can be enhanced by simply recycling the unexfoliated graphite particles. These results tell us that the C_G can be substantially enhanced by increasing the graphite concentration and extending the sonication time. Coleman et al. [26] ever prepared graphene with a very high concentration (up to 1.2 mg/mL) by sonicating graphite powder over an extending time scale (~460 h), but their work is quite time-consuming and is not appropriate for industrial-scale implementation. Herein, we define the "exfoliation efficiency" as the exfoliation yield per unit time [27]. The C_G scales with $\sqrt{t_s}$, it can be concluded that the efficiency is in inverse proportion to the $\sqrt{t_s}$ and thus reduces with the increase of exfoliation time. Furthermore, extending exfoliation time leads to reduction of the lateral size of graphene nanosheets [26]. Based on these discussions, it is not recommended to unilaterally prolong sonication time to give a higher concentration of graphene. In many application fields, large size, typically micron-sized, graphene sheets are highly demanded. In our study, the optimal sonication time is considered to be 2 h, since we can prepare mainly micron-sized graphene with a moderate concentration (~30 μg/mL) and reasonable exfoliation efficiency (0.075%/h).

During the liquid-phase exfoliation, the final centrifugation step plays a vital role in the preparation of stable graphene dispersions. Centrifugation leads to the precipitation of largish graphene flakes and unexfoliated graphite particles, while retaining graphene nanosheets in the supernatant. In the previous reports, it was found that the stability of graphene colloids could be significantly enhanced at higher centrifugation rates (ω) [21,28]. Higher centrifugation rate results in smaller lateral size. In this work, we also performed centrifugation process at different rotation rates to investigate the effects on the stability of graphene. Typical sedimentation curves of water-dispersed graphene are plotted in Fig. 3a, where the C_G is approximately amenable to first order exponential decay [29]. To quantitatively analyze the stability of graphene colloids, the C_G is fitted by the inset equation of Fig. 3a, $C_G/C_I = C_0/C_I+(1-C_0/C_I)e^{-t/\tau}$, where the C_I represents the initial concentration of graphene (thus prior to sedimentation), C_0 is the concentration of the stable phase, and the τ is the time constant. The fitting results are displayed in Table S1. Apparently, the stability of graphene, which can be illustrated by the value of C_0/C_I, is enhanced by increasing the ω. At 1500 rpm (319 g), the C_G decreased rapidly, indicating severe agglomeration within one week. In contrast, the C_G reduced steadily and eventually to 61% of the initial concentration at 2000 rpm (568 g), which suggests a much better stability. At 2500 rpm (888 g), the final value of C_0/C_I is further improved to ~69%, which means that most of the graphene flakes remain dispersed over long time scales [28]. Zeta potential reveals that a strong electrostatic repulsion force is responsible for the enhanced stability. The zeta potential of graphene at 2500 rpm is −40.7 mV, which exceeds the critical value

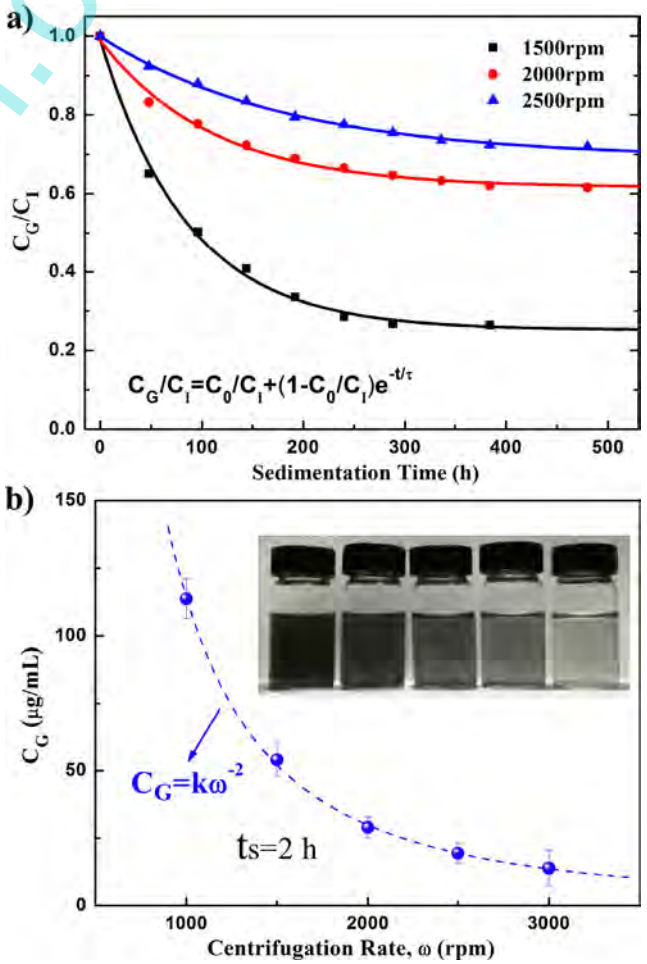

Fig. 3. (a) Sedimentation curves of graphene dispersions at different centrifugation rates. (b) Graphene concentration as a function of centrifugation rate. The inset shows a photograph of graphene dispersions prepared at different centrifugation rates (from left to right): 1000 rpm, 1500 rpm, 2000 rpm, 2500 rpm and 3000 rpm.

of 30 mV that can ensure a good stability. On the other hand, it has been reported that the concentration of graphene decreases with the increase of ω [19,21]. Accordingly in our study, the concentration is 113.69 μg/mL at 1000 rpm, but reduces to 13.80 μg/mL at 3000 rpm (Fig. 3b). Surprisingly, our fitting result shows that the C_G scales with ω^{-2} rather than ω^{-1}. This finding is consistent with the centrifugation theory, but is distinct from the results of a previous literature [26]. Considering stability, concentration and lateral size, we believe that the optimal centrifugation speed is 2000 rpm.

3.2. Morphology and quality of graphene

In order to systematically assess the morphology and quality of graphene, or the exfoliation degree of graphite, various characterizations were performed. Fig. 4a shows a typical TEM image of the as-exfoliated graphene nanosheets with diverse lateral sizes. It can be seen that several small flakes with lateral size of 200–600 nm are stacked on a large flake with lateral size of about 1 μm. The number of layers of the graphene flakes can be precisely counted through the HRTEM observation. The number of layers can be readily determined by counting the number of the dark lines at the folded edges. For instance, by directly counting the number of the dark lines, we can easily confirm that the observed graphene flake shown in Fig. 4b contains 4 layers. Despite a small amount of thick flakes (>8 layers), it is found that most graphene flakes are few-layered (2–7 layers). This result confirms the presence of thin graphene nanosheets, and thus the efficient exfoliation of graphite. The electron diffraction pattern (Fig. 4c) shows a hexagonal symmetry structure, indicating that the crystallinity of graphene structure is retained during the exfoliation process [30]. The asymmetric distribution of diffraction intensity may be attributed to the superposition of diffraction beams of upper and lower graphene layers. More TEM and HRTEM images are displayed in Figs. S3 and S4 of Supplementary Information, respectively.

Meanwhile, AFM can be employed to directly and precisely identify the thickness and the lateral size of graphene nanosheets. The height of the graphene flake shown in Fig. 5 is measured as ~1.7 nm, while the lateral size can be estimated as ~2 μm. Mica is applied as the substrate, and thus graphene flakes are often raised by extra several angstroms above the substrate [31], we herein regard this 1.7 nm-thick graphene sheet as 3–4 layers. We find many flakes to have a thickness of 1.5–3.5 nm and a lateral size ranging from 200 nm to 2 μm, suggesting that as-obtained graphene nanosheets are mainly few-layered and with a wide size distribution. The AFM data are in good agreement with the TEM analysis. Additional AFM images are shown in Fig. S5. In addition, in comparison with graphene flakes exfoliated in aqueous solution of NaOH with thickness ranging from several nanometers to several tens of nanometers [22], graphene sheets prepared by our method are much thinner, indicating a higher degree of exfoliation.

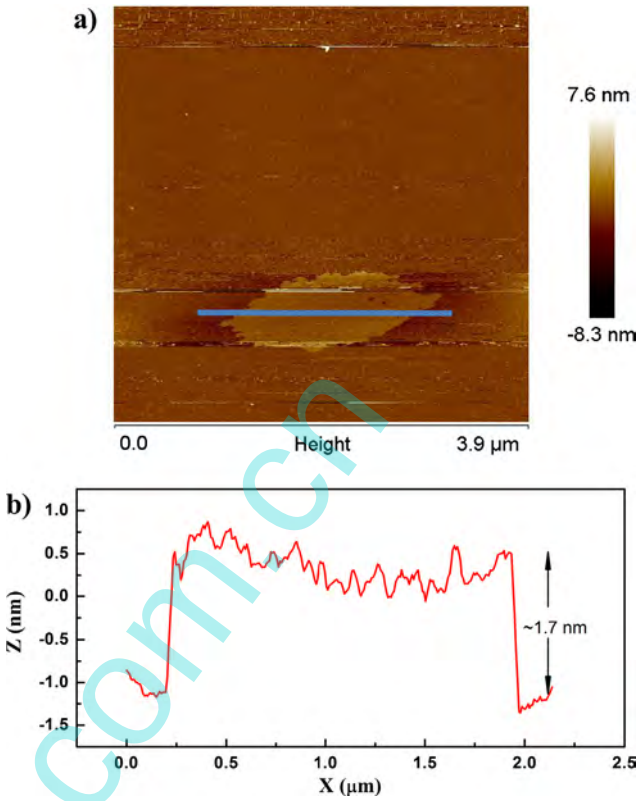

Fig. 5. (a) An AFM image of a graphene flake. (b) Corresponding height profile of the graphene flake.

XPS was performed to determine the chemical compositions of as-prepared samples and characterize the chemical status of elements in them. Survey spectra of pristine graphite and graphene are displayed in Fig. 6a. The oxygen content of graphene is 4.60%, which is a little higher than that of graphite (3.60%). As for the high-resolution spectra (Fig. 6b), the main peak of carbon element of graphene shows a very small positive shift, as compared with that of graphite (~284.8 eV). Peak fitting results reveal that carbon is bonded with oxygen, and the content of C—OH and C=O bonds slightly increases after exfoliation. These results can be attributed to the reaction of graphene edges with water and the in situ NH_3 reduction of the oxygenated functional groups formed at the edges [32,33]. See Table S2 for more details. However, no obvious peak of nitrogen (~400 eV) was observed, indicating that there is a very small amount of nitrogen bonding with carbon atoms.

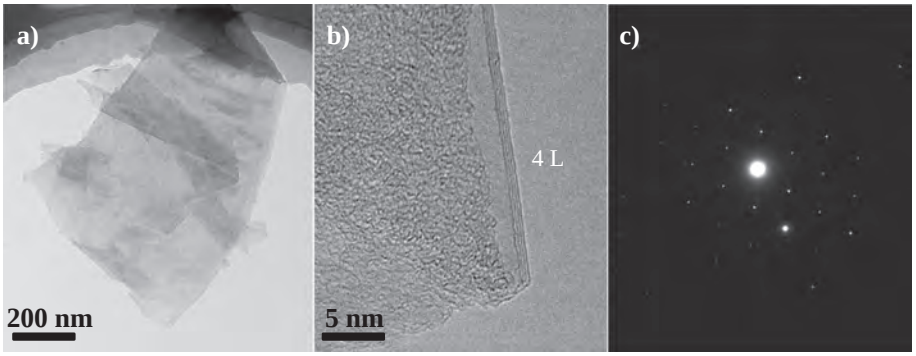

Fig. 4. (a) A typical TEM image of as-prepared graphene. (b) An HRTEM image showing a four-layer graphene. (c) An SAED pattern.

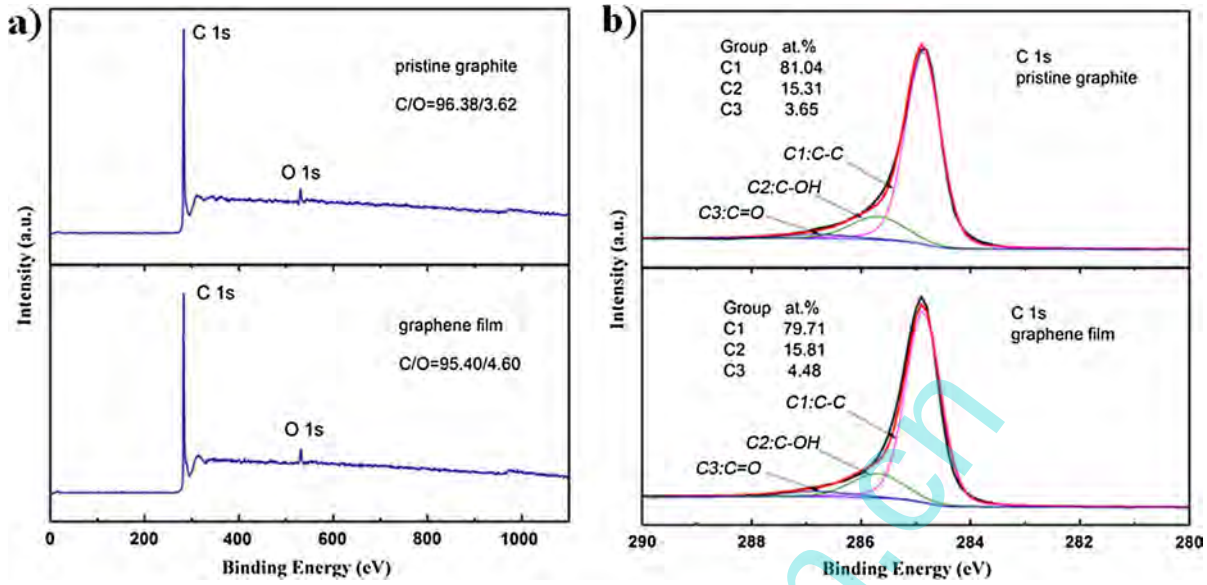

Fig. 6. XPS spectra of graphite and graphene. (a) Survey spectra of graphite and graphene film. (b) High-resolution spectra of C 1s.

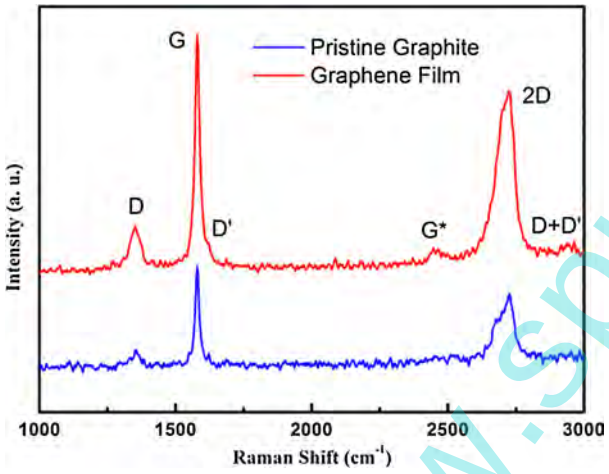

Fig. 7. Raman spectra of pristine graphite and graphene film.

As an essentially complementary characterization, Raman spectroscopy was performed to examine defect density and structural changes of pristine graphite and as-prepared graphene nanosheets. For comparison, the Raman spectra of pristine graphite and the graphene film prepared by vacuum filtration are displayed in Fig. 7. The D (~1350 cm^{-1}), G (~1580 cm-1) and D′ band (~1610 cm^{-1}) are first-order bands [34], while the G* (~2500 cm^{-1}), 2D (~2720 cm^{-1}) and D + D′ band (~2900 cm^{-1}) are second-order bands [35]. The shape of the 2D band is an indicator of the exfoliation degree of graphene. Apparently, the 2D band of graphite shows a remarkable shoulder, while no shoulder was found at the graphene film. This significant shape distinction illustrates that the nature of the graphene film is intrinsically different from pristine graphite, and confirms the exfoliation of graphene nanosheets from the graphite precursor [36,37]. On the other hand, the presence of D band indicates the existence of defects while the G band is attributed to the stretching of the C—C bond. The defect content can be characterized by the ratio of the intensity of D band to G band, I_D/I_G. These defects can be divided into two sorts: basal plane defects and edge defects [12,15]. Basal plane defects typically occur in GO or RGO, and lead to the broadening of G band [36,37]. However, remarkable broadening cannot be found in the spectrum of as-prepared graphene, suggesting that the current method introduces little basal plane defects. Considering that the size of graphene ranges from ~100 nm to 2 μm, and that the laser beam spot (1–2 μm) in the Raman spectroscopy will inevitably cover the edges, the presence of D band is probably due to edge defects rather than basal plane defects [38]. In addition, the value of I_D/I_G of graphene film is ~0.31, which is much lower than that of GO and RGO [15,39]. These analyses indicate that the basal plane of graphene nanosheets is not severely destroyed.

FTIR spectra of graphite and graphene are shown in Fig. S6. In the spectra, no prominent peaks are observed. A peak at 860 cm^{-1} is attributed to the inter-layer vibrational stretching of graphitic planes [40]. For graphene, this peak is relatively weak, indicating the efficient exfoliation. A peak at 1600 cm^{-1} is due to skeletal vibrations of graphitic domains [41]. In the spectrum of graphene, peaks at 1555 cm^{-1} and 1634 cm^{-1} can be ascribed to N—H bending vibration [42] and O—H bending vibration [43], respectively. In the XRD pattern of graphene (Fig. S7), a peak at 27.1° is corresponding to the (002) plane of the graphitic lattice. This indicates that the structure of graphene basal planes is not destroyed. To measure the electrical conductivity of graphene, we prepared a ~1.6 μm thick graphene film by vacuum filtration (Fig. S8). The conductivity is measured to be ~500 S/m. This value is comparable to that of KOH-activated microwave-exfoliated graphene oxide (a-MEGO) [44] and that of graphene exfoliated in pure water via temperature control [23].

3.3. Exfoliation and stabilizing mechanism

It has been widely accepted that pure water cannot be directly used as a solvent to exfoliate and disperse graphene. However, in our work where a small amount of aqueous ammonia (several tens of microliters) is added to the pure water, the exfoliation of graphite can be significantly enhanced, though the yield (<0.3%) is much lower than those liquid exfoliation methods using organic solvents or water/surfactant systems [17–19,24,26,28]. Hence, a critical issue we must concern is the effects of ammonia solution on the exfoliation behavior of graphite in water.

It is known that the layers in bulk graphite connect with each other via weak intersheet van der Waals forces (π–π stacking). In the process of sonication-assisted exfoliation, the collapses of numerous cavitation-induced bubbles eventually exert an intensive tensile force on the graphite flakes and make the exfoliation happen in a normal force dominated way [16]. On the other hand, if the surface energy of the solvent matches well with that of graphene, the energy barrier that needs to be overcome for an efficient exfoliation will be minimized [12]. This is the reason why some specific organic solvents such as NMP are favorable for exfoliation. Also, the addition of surfactants could remarkably reduce the surface energy of water, thereby resulting in a significant promotion of exfoliation. As for pure water, the surface energy is so high that the energy barrier is too high to overcome by sonication, leading to the extremely low exfoliation efficiency [18]. With this in mind, we attempt to use similar idea to explain why exfoliation of graphite occurs by adding aqueous ammonia. It is examined that the surface tension of concentrated ammonia solution (55.58 mJ/m^2) is indeed much lower than that of pure water, but the small amount of ammonia solution that added into water is hardly to affect the surface tension of water [45]. Hence, surface energy cannot account for the exfoliation behavior.

In the present study, we believe that the release of gaseous ammonia plays the key role for exfoliation of graphite. The composition investigations (Table S2) provide indirect evidence for the presence of ammonia. When ultrasonic cavitation occurs, bubble collapse occurs rapidly at some tiny areas and induces high local temperature (several thousand K) and pressure (several thousand atm) [46,47]. In ammonia-water system, the localized high temperature causes the rapid release of dissolved ammonia, promoting exfoliation. Water molecules tend to decompose to radicals and ions under such harsh conditions. Consequently, interactions between the active edge carbon atoms of graphene and these radicals or ions will occur. This makes the edges of graphene partially functionalized and thus oxygenated functional groups are formed [23,32]. In the literatures [48,49], the exfoliation process occurs when the steam pressure exceeds the interlayer van der Waals forces. However, the prerequisite of exfoliation is that there are cracks on basal planes of graphene or there is enough space between adjacent graphene layers (e.g. expanded graphite). In the present study, there is no enough space to ensure the infiltration of the precursor of ammonia gas. Wang et al. [33] achieved etching of graphene in the presence of oxygen and ammonia gas and attributed the etching process to the chemical reactions between graphene edges and the gas. Accordingly, we propose that in our work, a similar process happens. Specifically, the in situ NH_3 reduction of the oxygenated functional groups formed during oxidation happens and may open up these edges, as shown in Fig. 8. This effect can be called as a "wedge" effect and significantly reduces the exfoliation resistance. Theoretical works predict that NH_3 molecules physisorb to the plane of graphene without significant change of the band structure, although a very small charge transfer of f ~0.03–0.04e is predicted to happen [50,51]. The chemisorption of NH_3 molecules with a higher charge transfer of f = 0.18e is more likely to happen at defect sites due to a relatively low activation barrier [52]. At presence of pre-dissociated oxygen, the chemisorption is enhanced and becomes nearly spontaneous [52]. In our work, defects are mainly attached to the edges, so the in situ reduction energetically prefers to happen at edges instead of basal planes. On the other hand, from the mechanical perspective, ultrasonic cavitation results in a process of bubble formation, growth and collapse [53]. When the cavitaion bubbles collapse, micro-jets and shock waves act on the graphite surface instantly, resulting in compressive stress waves which propagate throughout the graphite body. When the compressive wave spreads to the free interface of graphite, a tensile stress wave will be reflected back to the body. This can be explained by the stress wave theory [54]. Collapses of numerous bubbles lead to an intensive tensile stress wave which acts as the driving force. The driving force is enough to peel off the graphene flakes, since the energy barrier between adjacent graphene flakes is significantly weakened by the wedge effect.

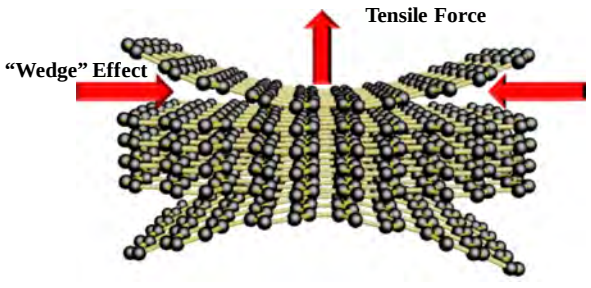

Fig. 8. Schematic presentations of exfoliation via a "wedge" effect and tensile force.

The last issue we should address is the stabilizing mechanism of graphene sheets. As shown in Fig. 3a, we find that higher centrifugation speed achieves better stability. Higher centrifugation speed leads to smaller flake size. As the centrifugation rate increases from 1500 rpm to 2500 rpm, the lateral size of majority of graphene sheets decreases from several micrometers to several hundred nanometers. The significant reduction of flake size leads to a much higher edge-to-area ratio and thus a much larger amount of edge carbon atoms that can react with water to from oxygen-containing groups. The ionization of these edge-attached groups renders edges negatively charged, generating repulsion and enhancing solubility [20,21]. On the other hand, because the van der Waals attractive force between smaller sheets is much smaller, much less repulsive force is needed to prevent smaller sheets from aggregation. When the flake size reduces to a certain extent, repulsive forces can overcome attractive forces and stabilize graphene colloids.

4. Conclusions

In this study, we report that graphene sheets can be efficiently exfoliated in water by adding a small amount of ammonia solution. Graphene with relatively high concentrations (over 0.05 mg/mL) can be stably dispersed in water via electrostatic repulsion. TEM, AFM, Raman, XPS, FTIR and XRD results demonstrate that the graphene sheets are of reasonably high quality. The chemical interaction of released ammonia with graphite plays an important role for exfoliation of graphene. We believe that our work gives new insights in producing and dispersing of graphene. The graphene dispersions synthesized by our method can be effectively used for inkjet printing and transparent electrodes.

Acknowledgements

This work was supported by the Special Funds for Co-construction Project of Beijing Municipal Commission of Education, the Fundamental Research Funds for the Central Universities, the Specialized Research Fund for the Doctoral Program of Higher Education (20131102110016), and the Beijing Natural Science Foundation (2132025).

Appendix A. Supplementary material

Supplementary data associated with this article can be found, in the online version, at http://dx.doi.org/10.1016/j.jcis.2017.04.070.

References

[1] C. Lee, X. Wei, J.W. Kysar, J. Hone, Measurement of the elastic properties and intrinsic strength of monolayer graphene, Science 321 (2008) 385–388.
[2] P. Avouris, Graphene: electronic and photonic properties and devices, Nano Letters 10 (2010) 4285–4294.
[3] A.A. Balandin, Thermal properties of graphene and nanostructured carbon materials, Nat. Mater. 10 (2011) 569–581.
[4] H. Dalir, Y. Xia, Y. Wang, X. Zhang, Athermal broadband graphene optical modulator with 35 Hz speed, ACS Photonics 3 (2016) 1564–1568.
[5] R. Raccichini, A. Varzi, S. Passerini, B. Scrosati, The role of graphene for electrochemical energy storage, Nat. Mater. 14 (2015) 271–279.
[6] S. Stankovich, D.A. Dikin, G.H.B. Dommett, K.W. Kohlhaas, E.J. Zimney, E.A. Stach, R.D. Piner, S.T. Nguyen, R.S. Ruoff, Graphene-based composite materials, Nature 442 (2006) 282–286.
[7] B.F. Machado, P. Serp, Graphene-based materials for catalysis, Catal. Sci. Technol. 2 (2012) 54–75.
[8] K.S. Novoselov, A.K. Geim, S.V. Morozov, D. Jiang, Y. Zhang, S.V. Dubonos, I.V. Grigorieva, A.A. Firsov, Electric field effect in atomically thin carbon films, Science 306 (2004) 666–669.
[9] Y. Zhang, L. Zhang, C. Zhou, Review of chemical vapor deposition of graphene and related applications, Acc. Chem. Res. 46 (2013) 2329–2339.
[10] K.V. Emtsev, F. Speck, T. Seyller, L. Ley, J.D. Riley, Interaction, growth, and ordering of epitaxial graphene on SiC{0001} surfaces: a comparative spectroscopy study, Phys. Rev. B: Condens. Matter Mater. Phys. 77 (2008) 155303.
[11] D.R. Dreyer, S. Park, C.W. Bielawski, R.S. Ruoff, The chemistry of graphene oxide, Chem. Soc. Rev. 39 (2010) 228–240.
[12] Y. Hernandez, V. Nicolosi, M. Lotya, F.M. Blighe, Z. Sun, S. De, I.T. McGovern, B. Holland, M. Byrne, Y.K. Gun'Ko, J.J. Boland, P. Niraj, G. Duesberg, S. Krishnamurthy, R. Goodhue, J. Hutchison, V. Scardasi, A.C. Ferrari, J.N. Coleman, High-yield production of graphene by liquid-phase exfoliation of graphite, Nat. Nanotechnol. 3 (2008) 563–568.
[13] D.B. Shinde, J. Brenker, C.D. Easton, R.F. Tabor, A. Neild, M. Majumder, Shear assisted electrochemical exfoliation of graphite to graphene, Langmuir 32 (2016) 3552–3559.
[14] C. Cheng, D. Li, Solvated graphenes: an emerging class of functional soft materials, Adv. Mater. 25 (2013) 13–30.
[15] S. Stankovich, D.A. Dikin, R.D. Piner, K.A. Kohlhaas, A. Kleinhammes, Y. Jia, Y. Wu, S.T. Nguyen, R.S. Ruoff, Synthesis of graphene-based nanosheets via chemical reduction of exfoliated graphite oxide, Carbon 45 (2007) 1558–1565.
[16] M. Yi, Z. Shen, A review on mechanical exfoliation for the scalable production of graphene, J. Mater. Chem. A 3 (2015) 11700–11715.
[17] J.N. Coleman, Liquid exfoliation of defect-free graphene, Acc. Chem. Res. 46 (2013) 14–22.
[18] M. Lotya, Y. Hernandez, P.J. King, R.J. Smith, V. Nicolosi, L.S. Karlsson, F.F.M. Blighe, S. De, Z. Wang, I.T. McGovern, G.S. Duesberg, J.N. Coleman, Liquid phase production of graphene by exfoliation of graphite in surfactant/water solutions, J. Am. Chem. Soc. 131 (2009) 3611–3620.
[19] M. Lotya, P.J. King, U. Khan, S. De, J.N. Coleman, High-concentration, surfactant-stabilized graphene dispersions, ACS Nano 4 (2010) 3155–3162.
[20] D. Li, M.B. Muller, S. Gilje, R.B. Kaner, G.G. Wallace, Processable aqueous dispersions of graphene nanosheets, Nat. Nanotechnol. 3 (2008) 101–105.
[21] M. Yi, Z. Shen, S. Liang, L. Liu, X. Zhang, S. Ma, Water can stably disperse liquid-exfoliated graphene, Chem. Commun. 49 (2013) 11059–11061.
[22] K.B. Ricardo, A. Sendecki, H. Liu, Surfactant-free exfoliation of graphene in aqueous solutions, Chem. Commun. 50 (2014) 2751–2754.
[23] J. Kim, S. Kwon, D.H. Cho, B. Kang, H. Kwon, Y. Kim, S.O. Park, G.Y. Jung, E. Shin, W.G. Kim, H. Lee, G.H. Ryu, M. Choi, T.H. Kim, J. Oh, S. Park, S.K. Kwak, S.W. Yoon, D. Byun, Z. Lee, C. Lee, Direct exfoliation and dispersion of two-dimensional materials in pure water via temperature control, Nat. Commun. 6 (2015) 8294.
[24] U. Khan, H. Porwal, A. O'Neill, K. Nawaz, P. May, J.N. Coleman, Solvent-exfoliated graphene at extremely high concentration, Langmuir 27 (2011) 9077–9082.
[25] E. Varrla, C. Backes, K.R. Paton, A. Harvey, Z. Gholamvand, J. McCauley, J.N. Coleman, Large-scale production of size-controlled mos_2 nanosheets by shear exfoliation, Chem. Mater. 27 (2015) 1129–1139.
[26] U. Khan, A. O'Neill, M. Lotya, S. De, J.N. Coleman, High-concentration solvent exfoliation of graphene, Small 6 (2010) 864–871.
[27] M. Yi, Z. Shen, Kitchen blender for producing high-quality few-layer graphene, Carbon 78 (2014) 622–626.
[28] M. Yi, Z. Shen, S. Ma, X. Zhang, A mixed-solvent strategy for facile and green preparation of graphene by liquid-phase exfoliation of graphite, J. Nanopart. Res. 14 (2012) 1003.
[29] V. Nicolosi, D. Vrbanic, A. Mrzel, J. McCauley, S. O'Flaherty, C. McGuinness, G. Compagnini, D. Mihailovic, W.J. Blau, J.N. Coleman, Solubility of $Mo_6S_{4.5}I_{4.5}$ nanowires in common solvents: a sedimentation study, J. Phys. Chem. B 109 (2005) 7124–7133.
[30] D. Rangappa, K. Sone, M. Wang, U.K. Gautam, D. Golberg, H. Itoh, M. Ichihara, I. Honma, Rapid and direct conversion of graphite crystals into high-yielding, good-quality graphene by supercritical fluid exfoliation, Chem.-Eur. J. 16 (2010) 6488–6494.
[31] P. Nemes-Incze, Z. Osvath, K. Kamaras, L.P. Biro, Anomalies in thickness measurements of graphene and few layer graphite crystals by tapping mode atomic force microscopy, Carbon 46 (2008) 1435–1442.
[32] N. Mitoma, R. Nouchi, K. Tanigaki, Photo-oxidation of graphene in the presence of water, J. Phys. Chem. C 117 (2013) 1453–1456.
[33] X. Wang, H. Dai, Etching and narrowing of graphene from the edges, Nat. Chem. 2 (2010) 661–665.
[34] A. Sadezky, H. Muckenhuber, H. Grothe, R. Niessner, U. Poschl, Raman microspectroscopy of soot and related carbonaceous materials: spectral analysis and structural information, Carbon 43 (2005) 1731–1742.
[35] A. Gupta, G. Chen, P. Joshi, S. Tadigadapa, P.C. Eklund, Raman scattering from high-frequency phonons in supported n-graphene layer films, Nano Lett. 6 (2006) 2667–2673.
[36] A.C. Ferrari, J.C. Meyer, V. Scardaci, C. Casiraghi, M. Lazzeri, F. Mauri, S. Piscanec, D. Jiang, K.S. Novoselov, S. Roth, A.K. Geim, Raman spectrum of graphene and graphene layers, Phys. Rev. Lett. 97 (2006) 187401.
[37] L.M. Malard, M.A. Pimenta, G. Dresselhaus, M.S. Dresselhaus, Raman spectroscopy in graphene, Phys. Rep. 473 (2009) 51–87.
[38] Z. Shen, J. Li, M. Yi, X. Zhang, S. Ma, Preparation of graphene by jet cavitation, Nanotechnology 22 (2011) 365306.
[39] S. Stankovich, R.D. Piner, X. Chen, N. Wu, S.T. Nguyen, R.S. Ruoff, Stable aqueous dispersions of graphitic nanoplatelets via the reduction of exfoliated graphite oxide in the presence of poly [sodium 4-styrenesulfonate], J. Mater. Chem. 16 (2006) 155–158.
[40] R.J. Nemanich, G. Lucovsky, S.A. Solin, Infrared active optical vibrations of graphite, Solid State Commun. 23 (1977) 117–120.
[41] S. Stankovich, R.D. Piner, S.T. Nguyen, R.S. Ruoff, Synthesis and exfoliation of isocyanate-treated graphene oxide nanoplatelets, Carbon 44 (2006) 3342–3347.
[42] D. Geng, S. Yang, Y. Zhang, J. Yang, J. Liu, R. Li, T.K. Sham, X. Sun, S. Ye, S. Knights, Nitrogen doping effects on the structure of graphene, Appl. Surf. Sci. 257 (2011) 9193–9198.
[43] Z. Tang, J. Zhang, X. Wang, Exfoliation of graphene from graphite and their self-assembly at the oil –water interface, Langmuir 26 (2010) 9045–9049.
[44] L.L. Zhao, X. Zhao, M.D. Stoller, Y. Zhu, H. Ji, S. Murali, Y. Wu, S. Perales, B. Clevenger, R.S. Ruoff, Highly conductive and porous activated reduced graphene oxide film for high-power supercapacitors, Nano Lett. 12 (2012) 1806–1812.
[45] H.H. King, J.L. Hall, G.C. Ware, A study of the density, surface tension, and adsorption in the water-ammonia system at 20°, J. Am. Chem. Soc. 52 (1930) 5128–5135.
[46] E.B. Flint, K.S. Suslick, The temperature of cavitation, Science 253 (1991) 1397–1399.
[47] W.B. McNamara, Y.T. Didenko, K.S. Suslick, Sonoluminescence temperatures during multi-bubble cavitation, Nature 401 (1999) 772–775.
[48] I. Janowska, K. Chizari, O. Ersen, S. Zafeiratos, D. Soubane, V.D. Costa, V. Speisser, C. Boeglin, M. Houlle, D. Begin, D. Plee, M.J. Ledoux, P.H. Cuong, Microwave synthesis of large few-layer graphene sheets in aqueous solution of ammonia, Nano Research 3 (2010) 126–137.
[49] Y.B. Tang, C.S. Lee, Z.H. Chen, G.D. Yuan, Z.H. Kang, L.B. Luo, H.S. Song, Y. Liu, Z. B. He, W.J. Zhang, I. Bello, S.T. Lee, High-quality graphenes via a facile quenching method for field-effect transistors, Nano Letters 9 (2009) 1374–1377.
[50] O. Leenaerts, B. Partoens, F.M. Peeters, Adsorption of H_2O, NH_3, CO, NO_2, and NO on graphene: a first-principles study, Phys. Rev. B 77 (2008) 125416.
[51] C.W. Bauschlicher, A. Ricca, Binding of NH_3 to graphite and to a (9,0) carbon nanotube, Phys. Rev. B 70 (2004) 115409.
[52] H.E. Romero, P. Joshi, A.K. Gupta, H.R. Gutierrez, M.W. Cole, S.A. Tadigadapa, P. C. Eklund, Adsorption of ammonia on graphene, Nanotechnology 20 (2009) 245501.
[53] T.J. Mason, J.P. Lorimer, Appl. Sonochem. 2002.
[54] L. Wang, Foundations of stress waves, 2007.